Electronic Supplementary Material (ESI) for Dalton Transactions.

Supplementary Information

Methyldisulfide groups enable the direct connection of air-stable metal bis(terpyridine) complexes to gold surfaces

Christina D.M. Trang, Thomas Saal, and Michael S. Inkpen*

Department of Chemistry, University of Southern California, Los Angeles, California 90089, United States

E-mail: inkpen@usc.edu

Contents

1. General Information

Synthetic Methods

All manipulations were carried out in oven-dried glassware under a nitrogen atmosphere using standard Schlenk line techniques, or inside of an OMNI-Lab 4-port glovebox (Vacuum Atmospheres Company, Hawthorne, CA, USA. No special precautions were taken to exclude air or moisture during workup unless otherwise stated. Dichloromethane was sparged with nitrogen and dried using a two-column solvent purification system packed with alumina (Pure Process Technologies, Nashua, NH, USA). *N*,*N*-Dimethylformamide (DMF) was purified by vacuum distillation, dried over 3Å molecular sieves, and stored under nitrogen. Other reaction solvents (sparged with nitrogen prior to use) and chemical regents were commercially available and used without further purification. 18.2 MΩ water was generated using an Arium® Mini Plus UV ultrapure water system (Sartorius AG, Goettingen, Germany). Deuterated solvents were purchased from Cambridge Isotope Laboratories, Inc., Cambridge Isotope Laboratories, Tewksbury, MA USA. Flash chromatography was performed using a Pure C-850 FlashPrep chromatography system and FlashPure EcoFlex flash cartridges (neutral alumina, irregular 50-75 μm particle size, 50-70 Å pore size; BUCHI Corporation, New Castle, DE, USA), or by hand using neutral alumina adjusted to Brockmann activity V (15% H_2O; Acros Organics, 50-200 μm particle size, 60 Å pore size). Suspensions were separated using a VanGuard V6500 centrifuge (Hamilton Bell, Montvale, NJ, USA).

^{1}H and ^{13}C{^{1}H} NMR spectra were recorded at room temperature on Varian VNMRS 500 (500 MHz), VNMRS 600 (600 MHz), or Mercury 400 (400 MHz) NMR spectrometers, unless otherwise stated. ^{1}H NMR data recorded in $CDCl_3$, MeCN-d_3, DMSO-d_6, and acetone-d_6 is referenced to residual internal C*H*Cl_3 (δ 7.26), C*H*D_2CN (δ 1.94), (C*H*D_2)(CD_3)SO (δ 2.50), and (C*H*D_2)(CD_3)CO (δ 2.05) solvent signals.[1] ^{13}C{^{1}H} NMR data recorded in $CDCl_3$ and MeCN-d_3 is referenced to internal *C*DCl_3 (δ 77.16) and *C*D_3CN (δ 1.32).[1] ^{1}H and ^{13}C{^{1}H} resonances were assigned where possible for new compounds using 2D correlation spectroscopy experiments. Mass spectrometry analyses were performed on a Waters Synapt G2-Si at the Mass Spectrometry Lab, University of Illinois Urbana-Champaign. Microanalyses were carried out using a Control Equipment Corp. CEC 440HA Elemental Analyzer at the Marine Science Institute, University of California Santa Barbara (found values are the average of two runs).

X-Ray Crystallography

*For **tpySSMe**, **FeSS**, **CoSS**:* X-ray intensity data were collected at 100 K on a Bruker APEX DUO 3-circle platform diffractometer, equipped with an APEX II CCD detector, using MoKα radiation (λ = 0.71073 Å, TRIUMPH curved-crystal monochromator) from a fine-focus tube. The structures were solved by intrinsic phasing and refined on F^2 using the Bruker APEX3 Software Package and ShelXle.[2–5] *For **ZnSS**:* X-ray intensity data were collected on a Rigaku XtaLAB Synergy, Dualflex, equipped with a HyPix-6000HE pixel array detector, using CuKα radiation (λ = 1.54184 Å) from microfocus sealed tube. The structure was solved using dual methods and refined on F^2 using ShelXle.[3–6] All non-hydrogen atoms were refined anisotropically. Further crystallographic details can be obtained from the Cambridge Crystallographic Data Centre (CCDC, 12 Union Road, Cambridge, CB2 1EZ, UK (Fax: (+44) 1223–336–033; e-mail: deposit@ccdc.cam.ac.uk) on quoting the deposition no. CCDC 2220466-2220469.

Electrochemical Methods

Electrochemical measurements were performed under an argon atmosphere using a CHI760E bipotentiostat (CH Instruments, Austin, TX, USA) with argon or nitrogen-sparged 0.1 M tetrabutylammonium hexafluorophosphate (NBu_4PF_6) MeCN or CH_2Cl_2 solutions (using non-anhydrous solvents). Unless otherwise stated, solution voltammograms were obtained in MeCN (scan rate = 0.1 V s^{-1}), and surface voltammograms in CH_2Cl_2 (scan rate = 1 V s^{-1}). Plotted voltammograms are not corrected for iR_s unless otherwise stated. Solution studies employed glassy carbon disc working electrodes (Ø = 3 mm, CH Instruments), mechanically polished using an alumina slurry prior to use. Pt wire reference and counter electrodes were cleaned by annealing in an oxyhydrogen flame. Analyte solutions were between 0.1-1 mM. Potentials are reported relative to $[Cp_2Fe]^+/[Cp_2Fe]$ (unless otherwise stated), measured against internal Cp_2Fe or Cp^*_2Fe references as appropriate.

Gold disk electrodes (⌀ = 2 mm; CH Instruments) used for SAM studies were first cleaned by mechanical polishing using an alumina slurry (0.05 μm). After thorough rinsing with 18.2 MΩ water, they were agitated in piranha solution (conc. H_2SO_4−30% H_2O_2, 3:1 w/w) for 1 min, rinsed with 18.2 MΩ water and ethanol, then immersed in ethanol for ≥20 min.[7] After cleaning, electrodes were immediately immersed in 1 mM solutions of analyte in MeCN for ≥18 h to form SAMs,

unless otherwise stated. Prior to electrochemical measurements, the electrodes were removed from the SAM formation solutions and washed thoroughly with MeCN then the solvent used for electrochemical measurements (e.g., CH_2Cl_2).

SAMs of **CoSS** and **CoSH** formed under an inert nitrogen atmosphere were prepared inside of an OMNI-Lab 4-port glovebox (Vacuum Atmospheres Company, Hawthorne, CA, USA). Clean gold disc electrodes were pumped into the glovebox, then immersed for 18-24 h in 1 mM **CoSS** or **CoSH** solutions in MeCN (dried over 3Å sieves, sparged with nitrogen). After emersion, the electrodes were washed thoroughly with MeCN and CH_2Cl_2 (dried over 3Å sieves, sparged with nitrogen) then integrated into a custom air-tight three electrode cell comprising Pt counter and reference electrodes. A solution of 0.1 M NBu_4PF_6 in CH_2Cl_2 was added, then the sealed cell was removed from the glovebox to perform electrochemical measurements.

The average real surface area of the gold electrodes used in these experiments was determined by measuring cyclic voltammograms between −0.2 and 1.6 V versus Ag/AgCl in aqueous 0.1 M H_2SO_4. The area was calculated from the charge obtained for the gold reduction peak (first cycle, using a scan rate of 5 V s^{-1}) divided by the reference charge of 390 μC cm^{-2} for reduction of an oxide monolayer on polycrystalline gold.[8,9] From two sets of three electrodes (prepared and measured on different days) we obtained a real surface area of 0.073 ± 0.012 (1 s.d.) cm^2, corresponding to a roughness factor of ~2.3.

Gold-on-glass substrates for selected electrochemical studies were prepared by evaporation of 5 nm chromium (Angstrom Engineering Inc., ON, Canada) then 200 nm gold (99.9985%, Alfa Aesar) onto <1 cm^2 glass substrates cut from 3" × 1" × 1 mm microscope slides (Premium Plain VWR Micro Slides, VWR International, LLC, USA), using a COVAP Physical Vapor Deposition System (Angstrom Engineering Inc., ON, Canada) applied exclusively for metal evaporation. Prior to metal evaporation, glass substrates were cleaned by boiling in a 20% nitric acid bath for 10 minutes, rinsed with 18.2 MΩ water, then dried and stored at 120 °C. Gold-on-glass substrates were used without further processing on the same day as metal evaporation.

2. Synthetic Details

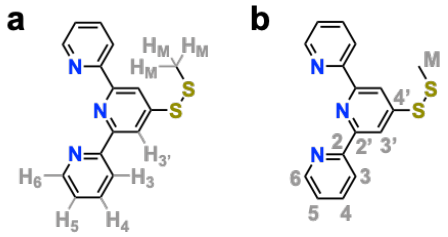

Figure S1. NMR labelling scheme for terpyridine **(a)** ^{1}H and **(b)** ^{13}C{^{1}H} resonances. Resonances for **tpySH** and **CoSH** follow the same scheme but omit H_M and C_M.

*4'-Methyldisulfide-2,2':6,2''-terpyridine (**tpySSMe**)*

This synthetic procedure was adapted from literature methods.[10,11] Anhydrous DMF (72 mL) was added to 4'-chloro-2,2':6',2"-terpyridine (0.993 g, 3.71 mmol) and NaSH · xH_2O (≥60%; 5.369 g, ≥57.5 mmol) in a 200 mL Schlenk flask equipped with a stir bar and condenser. The yellow mixture was heated to reflux for 4 h with stirring, cooled to room temperature, then filtered through a glass fritted filter. Solvent was removed by rotary evaporation and the yellow residue re-dissolved in water (50 mL) whereby an aqueous 1 M HCl solution was added dropwise to precipitate the product from solution. The suspended solid was isolated by filtration, washed with water, then dried under vacuum to yield 2,2':6',2"-terpyridine-4'-thiol (**tpySH**) as a bright yellow solid (0.905 g, 92%). Spectroscopic data was generally consistent with previous reports.[10] ^{1}H NMR (DMSO-d_6, 400 MHz): ***δ*** (ppm) 7.63 (m, 2H), 8.05 (td, 2H, J = 1.7 and 7.9 Hz), 8.14 (br s, 2H), 8.44 (d, 2H, J = 8.0 Hz), 8.85 (d, 2H, J = 4.7 Hz), −SH/−NH proton not observed. HR-MS (ESI+) *m/z*: 266.0751 ($[M+H]^+$ calc. for $C_{15}H_{12}N_3S$ 266.0752).

Water (4 mL) was added to **tpySH** (0.994 g, 3.75 mmol) and NaOH (0.154 g, 3.85 mmol) in a Schlenk flask equipped with a stir bar. After full dissolution of solid materials, S-methyl methanethiosulfonate (0.35 mL, 3.7 mmol) was added dropwise via syringe with stirring, forming a light-yellow suspension. After stirring at room temperature for 2 h, the opaque yellow mixture was extracted with CH_2Cl_2 (3 × 10 mL), dried with $MgSO_4$, and filtered. Solvent was removed under vacuum, whereby the crude product (yellow oil) was adsorbed onto Celite and purified by column chromatography (alumina V; hexanes/ethyl acetate [1:0 → 9:1 v/v]). Evaporation of selected fractions provided **tpySSMe** as a white solid (0.987 g, 86% yield). Single crystals suitable for X-ray diffraction were grown from vapor diffusion of pentane into a $CHCl_3$ solution. ^{1}H NMR

($CDCl_3$, 600 MHz): ***δ*** (ppm) 2.51 (s, 3H, H_M), 7.30 (m, 2H, H_5), 7.81 (td, 2H, J = 1.6 and 7.6 Hz, H_4), 8.57 (d, 2H, J = 7.9 Hz, H_3), 8.61 (s, 2H, $H_{3'}$), 8.69 (d, 2H, J = 4.68 Hz, H_6). ^{1}H NMR (MeCN-d_3, 400 MHz): ***δ*** (ppm) 2.55 (s, 3H), 7.44 (m, 2H), 7.95 (td, 2H, J = 1.7 and 7.9 Hz), 8.62 (s, 2H), 8.64 (d, 2H, J = 8.0 Hz), 8.70 (d, 2H, J = 4.7 Hz). ^{13}C{^{1}H} NMR ($CDCl_3$, 150 MHz): ***δ*** (ppm) 23.06 (C_M), 117.22 ($C_{3'}$), 121.46 (C_3), 124.00 (C_5), 136.85 (C_4), 149.21 (C_6), 150.86 ($C_{4'}$), 155.57 (C_2), 155.72 ($C_{2'}$). HR-MS (ESI+) *m/z*: 312.0626 ($[M+H]^+$ calc. for $C_{16}H_{14}N_3S_2$: 312.0629). Anal. Calc. for $C_{16}H_{13}N_3S_2$: C, 61.71; H, 4.21; N, 13.49%. Found: C, 61.61; H, 4.38; N, 13.14%.

*[Fe(**tpySSMe**)$_2$][PF$_6$]$_2$ (**FeSS**)*

This synthetic procedure was adapted from literature methods.[12] Methanol (7.5 mL) was added to **tpySSMe** (0.115 g, 0.370 mmol) and $FeCl_2 \cdot 4H_2O$ (0.038 g, 0.19 mmol) in a Schlenk flask equipped with a stir bar. The resulting dark purple solution was stirred for 1 h, then NH_4PF_6 (0.300 g, 1.85 mmol) in H_2O (1 mL) was added to precipitate the PF_6^- salt. After stirring for 10 min the suspension was centrifuged, the supernatant discarded, and the precipitate washed with additional H_2O to remove residual NH_4PF_6. Remaining solid material was dissolved in a minimum quantity of MeCN (~2 mL) then reprecipitated using excess diethyl ether (~10 mL). The suspension was again separated by centrifugation, washing the precipitate with additional diethyl ether to remove residual solvents and uncoordinated ligand. The isolated solid material was dried under vacuum to provide **FeSS** as a deep purple powder (0.165 g, 92% yield). Single crystals suitable for X-ray diffraction were grown by vapor diffusion of diethyl ether into a MeCN solution. ^{1}H NMR (MeCN-d_3, 500 MHz): ***δ*** (ppm) 2.83 (s, 6H, H_M), 7.09 (m, 4H, H_5), 7.16 (d, 4H, J = 5.6 Hz, H_6), 7.89 (td, 4H, J = 1.3 and 7.8 Hz, H_4), 8.53 (d, 4H, J = 7.9 Hz, H_3), 9.02 (s, 4 H, $H_{3'}$). ^{13}C{^{1}H} NMR (MeCN-d_3, 125 MHz): ***δ*** (ppm) 23.55 (C_M), 120.61 ($C_{3'}$), 125.05 (C_3), 128.45 (C_5), 139.69 (C_4), 153.85 ($C_{4'}$), 154.32 (C_6), 158.44 (C_2), 160.60 ($C_{2'}$). HR-MS (ESI+) *m/z*: 339.0225 ($[M]^{2+}$ calc. for $C_{32}H_{26}FeN_6S_4$: 339.0226). Anal. Calc. for $C_{32}H_{26}F_{12}FeN_6P_2S_4$: C, 39.68; H, 2.71; N, 8.68%. Found: C, 39.71; H, 2.64; N, 9.11%.

*[Co(**tpySSMe**)$_2$][PF$_6$]$_2$ (**CoSS**)*

These representative synthetic procedures were adapted from literature methods.[13,14] <u>*Method A:*</u> A mixture of MeOH (10 mL), $Co(OAc)_2 \cdot 4H_2O$ (0.064 g, 0.257 mmol), and **tpySSMe** (0.157 g, 0.504 mmol) was stirred at room temperature for 2 h. The resulting orange-brown solution was reduced in volume by rotary evaporation, whereby a solution of KPF_6 (0.429 g, 2.33 mmol) in water (5

mL) was added to precipitate the PF_6^- salt. The suspended solid was purified by centrifugation following the method described above for **FeSS**, providing **CoSS** as a dark orange powder (0.172 g, 70% yield). Single crystals suitable for X-ray diffraction were grown by vapor diffusion of diethyl ether into a MeCN solution. ^{1}H NMR (MeCN-d_3, 400 MHz): ***δ*** (ppm) 6.17 (s, 6H), 8.32 (s, 4H), 34.38 (s, 4H), 54.46 (s, 4H), 61.16 (s, 4H), 102.44 (br s, 4H). HR-MS (ESI+) *m/z*: 340.5213 ($[M]^{2+}$ calc. for $C_{32}H_{26}CoN_6S_4$: 340.5217). Anal. Calc. for $C_{32}H_{16}CoF_{12}N_6P_2S_4$: C, 39.55; H, 2.70; N, 8.65%. Found: C, 39.16; H, 2.60; N, 8.42%.

Method B: A mixture of $CoCl_2 \cdot 6H_2O$ (0.059 g, 0.248 mmol) and **tpySSMe** (0.158 g, 0.509 mmol) in MeOH (10 mL) was stirred at room temperature for 1 h, providing an orange-brown solution. Solvent was removed by rotary evaporation to yield a dark red-orange solid. The crude product was purified via column chromatography (alumina V, sample loaded in a minimum amount of solvent), collecting the dark red fraction that elutes with 10% MeOH in CH_2Cl_2. The solid residue obtained after solvent removal by rotary evaporation was re-dissolved in MeOH (5 mL), whereby a solution of KPF_6 (0.470 g, 2.55 mmol) in water (20 mL) was added to precipitate the PF_6^- salt. The suspended solid was purified by centrifugation following the method described above for **FeSS**, providing **CoSS** as a dark orange powder (0.101 g, 42% yield). Spectroscopic data matched that for samples prepared via *Method A*.

*[Co(**tpySSMe**)$_2$][PF$_6$]$_3$ (**CoSS^{3+}**)*

A solution of $AgPF_6$ in acetone (0.52 mL, 0.28 M, 0.15 mmol; stored in the absence of light) was added to an orange solution of **CoSS** (0.073 g, 0.075 mmol) in acetone (1 mL), resulting in an immediate colour change to dark green/brown. The silver precipitate was removed by syringe filtration (PTFE membrane, 0.2 μm pore size) to provide a yellow-orange solution. Removal of solvent under vacuum yielded **CoSS^{3+}** as a yellow-orange solid (0.082 g, quant. yield). ^{1}H NMR (MeCN-d_3, 400 MHz): ***δ*** (ppm) 2.83 (s, 6H, H_M), 7.36 (dd, 4H, J = 0.9 and 5.8 Hz, H_6), 7.45 (m, 4H, H_5), 8.23 (td, 4H, J = 1.4 and 7.9 Hz, H_4), 8.63 (dd, 4H, J = 1.1 and 8.0 Hz, H_3), 9.07 (s, 4H, $H_{3'}$). ^{13}C{^{1}H} NMR (MeCN-d_3, 150 MHz): ***δ*** (ppm) 23.44 (C_M), 123.96 ($C_{3'}$), 128.38 (C_3), 132.02 (C_5), 144.04 (C_4), 153.55 (C_6), 155.85 ($C_{2'}$), 156.62 (C_2), 164.76 ($C_{4'}$). HR-MS (ESI+) *m/z*: 227.0140 ($[M]^{3+}$ calc. for $C_{32}H_{26}CoN_6S_4$: 227.0145).

*[Co(**tpySH**)$_2$][PF$_6$]$_2$ (**CoSH**)*

This procedure was adapted from the one used to prepare **CoSS**, with the strict exclusion of air during both reaction and workup. MeOH (18 mL) was added to a Schlenk flask containing $CoCl_2 \cdot 6H_2O$ (0.101 g, 0.424 mmol) and **tpySH** (0.243 g, 0.916 mmol), resulting in a dark orange solution that was stirred at room temperature for 1 h. The solvent was reduced to ~1/4 of its volume under vacuum, whereby KPF_6 (0.842 g, 4.57 mmol) in H_2O (25 mL) was added to precipitate the PF_6^- salt. The orange precipitate was cannula filtered then washed with degassed H_2O (2 × 10 mL). Solid material was dissolved in MeCN (~5 mL) then precipitated by addition of ether (~25 mL). This suspension was cannula filtered and washed with ether (2 × 10 mL) then dried under vacuum overnight. The flask was transferred to a glovebox whereby **CoSH** was isolated as a brown-orange solid (0.186 g, 50%). ^{1}H NMR (MeCN-d_3, 500 MHz): ***δ*** (ppm) 7.64 (s, 4H), 11.33 (s, 2H), 34.78 (s, 4H), 62.23 (s, 4H), 64.61 (s, 4H), 106.65 (s, 4H). HR-MS (ESI+) m/z: 294.5340 ($[M]^{2+}$ calc. for $C_{30}H_{22}N_6S_2Co$: 294.5340). Anal. Calc. for $C_{32}H_{26}F_{12}N_6P_2S_4Co$ C, 40.97; H, 2.52; N, 9.56%. Found: C, 40.62; H, 2.55; N, 9.45%.

*[Zn(**tpySSMe**)$_2$][PF$_6$]$_2$ (**ZnSS**)*

This synthetic procedure was adapted from literature methods.[15] A solution of $Zn(OAc)_2 \cdot 2H_2O$ (0.043 g, 0.20 mmol) in MeOH (2 mL) was added to a solution of **tpySSMe** (0.123 g, 0.395 mmol) in CH_2Cl_2 (4 mL). The pale-yellow mixture was stirred at room temperature for 20 h, whereby solvent was removed by rotary evaporation. The crude residue was dissolved in water (~5 mL), then excess KPF_6 (0.321 g, 1.74 mmol) was added to precipitate a yellow solid. This precipitate was purified by centrifugation following the method described above for **FeSS**, providing **ZnSS** as an off-white solid (0.072 g, 37% yield). Single crystals suitable for X-ray diffraction were grown by vapor diffusion of diethyl ether into a MeCN solution. ^{1}H NMR (MeCN-d_3, 400 MHz): ***δ*** (ppm) 2.73 (s, 6H, H_M), 7.40 (m, 4H, H_5), 7.82 (d, 4H, J = 5.1 Hz, H_6), 8.15 (t, 4H, J = 8.0 Hz, H_4), 8.60 (d, 4H, J = 8.1 Hz, H_3), 8.83 (s, 4H, $H_{3'}$). ^{13}C{^{1}H} NMR (MeCN-d_3, 150 MHz): ***δ*** (ppm) 23.35 (C_M), 119.99 ($C_{3'}$), 124.27 (C_3), 128.68 (C_5), 142.27 (C_4), 148.41 (C_2), 149.15 (C_6), 150.13 ($C_{2'}$), 160.67 ($C_{4'}$). HR-MS (ESI+) *m/z*: 343.0188 ($[M]^{2+}$ calc. for $C_{32}H_{26}N_6S_4Zn$: 343.0197). Anal. Calc. for $C_{32}H_{26}F_{12}N_6P_2S_4Zn$: C, 39.29; H, 2.68; N, 8.59%. Found: C, 38.91; H, 2.44; N, 8.64%.

3. X-Ray Crystallography

Table S1. Sample and crystal data for **tpySSMe**.

Chemical formula	$C_{16}H_{13}N_3S_2$	
Formula weight	311.41 g/mol	
Temperature	100(2) K	
Wavelength	1.54178 Å	
Crystal size	0.101 x 0.146 x 0.254 mm	
Crystal habit	clear colourless blade	
Crystal system	monoclinic	
Space group	P 1 2_1/c 1	
Unit cell dimensions	a = 8.8399(2) Å	α = 90°
	b = 15.3680(3) Å	β = 96.1950(10)°
	c = 10.8169(2) Å	γ = 90°
Volume	1460.91(5) $Å^3$	
Z	4	
Density (calculated)	1.416 g/cm^3	
Absorption coefficient	3.260 mm^{-1}	
F(000)	648	

Table S2. Data collection and structure refinement for **tpySSMe**.

Diffractometer	Bruker APEX DUO
Radiation source	IμS microsource, CuKα
Theta range for data collection	5.02 to 70.13°
Index ranges	-10<=h<=10, -18<=k<=17, -13<=l<=12
Reflections collected	23417
Independent reflections	2773 [R(int) = 0.0374]
Coverage of independent reflections	99.8%
Absorption correction	multi-scan
Max. and min. transmission	0.753 and 0.618
Structure solution technique	direct methods
Structure solution program	SHELXTL XT 2014/5 (Bruker AXS, 2014)
Refinement method	Full-matrix least-squares on F^2
Refinement program	SHELXTL XL 2014/7 (Bruker AXS, 2014)
Function minimized	$\Sigma\, w(F_o^2 - F_c^2)^2$
Data / restraints / parameters	2773 / 0 / 191
Goodness-of-fit on F^2	1.075
Δ/σ_{max}	0.001
Final R indices	2572 data; I>2σ(I) $R_1 = 0.0289$, $wR_2 = 0.0797$
	all data $R_1 = 0.0313$, $wR_2 = 0.0817$
Weighting scheme	$w=1/[\sigma^2(F_o^2)+(0.0420P)^2+0.8770P]$ where $P=(F_o^2+2F_c^2)/3$
Largest diff. peak and hole	0.366 and -0.366 eÅ^{-3}
R.M.S. deviation from mean	0.049 eÅ^{-3}

Table S3. Sample and crystal data for **FeSS**.

Chemical formula	$C_{34}H_{29}F_{12}FeN_7P_2S_4$	
Formula weight	1009.67 g/mol	
Temperature	100 (2) K	
Wavelength	1.54178 Å	
Crystal size	0.044 x 0.183 x 0.270 mm	
Crystal habit	clear red prism	
Crystal system	monoclinic	
Space group	P 1 2_1 1	
Unit cell dimensions	a = 8.7953(2) Å	α = 90°
	b = 33.8428(8) Å	β = 92.314(2)°
	c = 14.0963(3) Å	γ = 90°
Volume	4192.45(16) $Å^3$	
Z	4	
Density (calculated)	1.600 g/cm^3	
Absorption coefficient	6.322 mm^{-1}	
F(000)	2128	

Table S4. Data collection and structure refinement for **FeSS**.

Diffractometer	Bruker APEX DUO
Radiation source	IμS microsource, CuKα
Theta range for data collection	2.61 to 70.07°
Index ranges	-10<=h<=10, 0<=k<=40, 0<=l<=17
Reflections collected	7951
Independent reflections	7951 [R(int) = 0.1455]
Coverage of independent reflections	98.1%
Absorption correction	multi-scan
Max. and min. transmission	0.753 and 0.527
Structure solution technique	direct methods
Structure solution program	SHELXL 2014/4 (Bruker AXS, 2014)
Refinement method	Full-matrix least-squares on F^2
Refinement program	SHELXL 2014/7 (Bruker AXS, 2014)
Function minimized	$\Sigma\, w(F_o^2 - F_c^2)^2$
Data / restraints / parameters	7951 / 101 / 1118
Goodness-of-fit on F^2	1.037
Δ/σ_{max}	0.010
Final R indices	6858 data; I>2σ(I) $R_1 = 0.0618$, $wR_2 = 0.1342$
	all data $R_1 = 0.0807$, $wR_2 = 0.1416$
Weighting scheme	$w=1/[\sigma^2(F_o^2)+(0.0535P)^2+11.3694P]$ where $P=(F_o^2+2F_c^2)/3$
Absolute structure parameter	0.490(16)
Largest diff. peak and hole	0.540 and -0.453 eÅ^{-3}
R.M.S. deviation from mean	0.101 eÅ^{-3}

Table S5. Sample and crystal data for **CoSS**.

Chemical formula	$C_{38}H_{35}CoF_{12}N_9P_2S_4$	
Formula weight	1094.86 g/mol	
Temperature	100 (2) K	
Wavelength	1.54178 Å	
Crystal size	0.064 x 0.142 x 0.267 mm	
Crystal habit	clear dark purple-red blade-like	
Crystal system	monoclinic	
Space group	P 1 2_1/c 1	
Unit cell dimensions	a = 8.9247 (3) Å	α = 90°
	b = 36.9029(12) Å	β = 93.753(2)°
	c = 13,7769(5) Å	γ = 90°
Volume	4527.7(3) $Å^3$	
Z	4	
Density (calculated)	1.606 g/cm^3	
Absorption coefficient	6.185 mm^{-1}	
F(000)	2220	

Table S6. Data collection and structure refinement for **CoSS**.

Diffractometer	Bruker APEX DUO
Radiation source	IμS microsource, CuKα
Theta range for data collection	2.39 to 69.32°
Index ranges	-10<=h<=10, -42<=k<=44, -16<=l<=16
Reflections collected	48292
Independent reflections	8258 [R(int) = 0.1078]
Coverage of independent reflections	97.3%
Absorption correction	multi-scan
Max. and min. transmission	0.637 and 0.441
Structure solution technique	direct methods
Structure solution program	SHELXL 2014/4 (Bruker AXS, 2014)
Refinement method	Full-matrix least-squares on F^2
Refinement program	SHELXL 2014/7 (Bruker AXS, 2014)
Function minimized	$\Sigma\, w(F_o^2 - F_c^2)^2$
Data / restraints / parameters	8258 / 145 / 613
Goodness-of-fit on F^2	1.163
Δ/σ_{max}	0.003
Final R indices	6858 data; I>2σ(I) $R_1 = 0.0851$, $wR_2 = 0.1886$
	all data $R_1 = 0.1061$, $wR_2 = 0.1973$
Weighting scheme	$w=1/[\sigma^2(F_o^2)+33.7607P]$ where $P=(F_o^2+2F_c^2)/3$
Largest diff. peak and hole	0.573 and -0.573 eÅ^{-3}
R.M.S. deviation from mean	0.108 eÅ^{-3}

Table S7. Sample and crystal data for **ZnSS**.

Chemical formula	$C_{32}H_{26}F_{12}N_6P_2S_4Zn$	
Formula weight	978.14 g/mol	
Temperature	100.00(11) K	
Wavelength	1.54184 Å	
Crystal size	0.19 x 0.11 x 0.04 mm	
Crystal habit	clear pale-yellow plates	
Crystal system	monoclinic	
Space group	P 1 2_1/c 1	
Unit cell dimensions	a = 9.0282(2) Å	α = 90°
	b = 9.5422(2) Å	β = 94.579(2)°
	c = 43.8494(7) Å	γ = 90°
Volume	3765.52(13) $Å^3$	
Z	4	
Density (calculated)	1.725 g/cm^3	
Absorption coefficient	4.657 mm^{-1}	
F(000)	1968	

Table S8. Data collection and structure refinement for **ZnSS**.

Diffractometer	XtaLAB Synergy, Dualflex, HyPix
Radiation source	micro-focus sealed X-ray tube, CuKα
Theta range for data collection	4.046 to 80.165°
Index ranges	-11<=h<=11, -8<=k<=12, -56<=l<=55
Reflections collected	33496
Independent reflections	7704 [R(int) = 0.0956]
Coverage of independent reflections	98.2%
Absorption correction	multi-scan
Max. and min. transmission	1.000 and 0.795
Structure solution technique	dual methods
Structure solution program	SHELXL 2014/5 (Sheldrick, 2014)
Refinement method	Full-matrix least-squares on F^2
Refinement program	SHELXL 2017/1 (Sheldrick, 2015)
Function minimized	$\Sigma\, w(F_o^2 - F_c^2)^2$
Data / restraints / parameters	7704 / 137 / 609
Goodness-of-fit on F^2	1.029
Δ/σ_{max}	0.002
Final R indices	5993 data; I>2σ(I) $R_1 = 0.0734$, $wR_2 = 0.1888$
	all data $R_1 = 0.0925$, $wR_2 = 0.2032$
Weighting scheme	$w=1/[\sigma^2(F_o^2)+(0.1017P)^2+13.4453P]$ where $P=(F_o^2+2F_c^2)/3$
Largest diff. peak and hole	1.683 and -1.064 eÅ^{-3}
R.M.S. deviation from mean	0.114 eÅ^{-3}

4. Electrochemistry

Solution Voltammetry

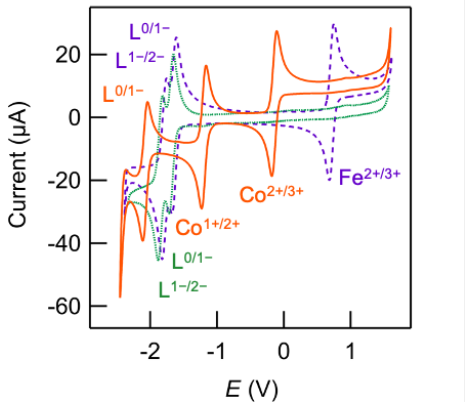

Figure S2. Overlaid solution cyclic voltammograms of parent [M(**tpy**)$_2$](PF$_6$)$_2$ complexes, showing salient features. M = Fe (purple dashed, current scaled by 0.6), Co (orange solid), Zn (green dotted). Features assigned based on previous reports.[16]

Table S9. Selected solution electrochemical parameters for metal bis(terpyridine) complexes.[a]

entry	complex	process	$E_{1/2}$	ΔE_p	E_{pa}	E_{pc}	I_{pa}/I_{pc}
1	[Fe(tpy)$_2$][PF$_6$]$_2$	$M^{2+/3+}$	0.716	0.068	0.750	0.682	1.10
2	**FeSS**	$M^{2+/3+}$	0.683	0.066	0.716	0.650	1.00
3	[Co(tpy)$_2$][PF$_6$]$_2$	$M^{2+/3+}$	−0.143	0.063	−0.112	−0.175	1.00
		$M^{1+/2+}$	−1.187	0.059	−1.158	−1.217	0.96
4	**CoSS**	$M^{2+/3+}$	−0.152	0.067	−0.119	−0.186	0.99

[a] Conditions: scan rate 0.1 V s^{-1}; working electrode, glassy carbon; reference and counter electrodes, Pt; electrolyte, MeCN−0.1 M Bu$_4$NPF$_6$. All potentials in V, corrected for iR_s and reported relative to FcH/[FcH]$^+$. $\Delta E_p = | E_{pa} - E_{pc} |$.

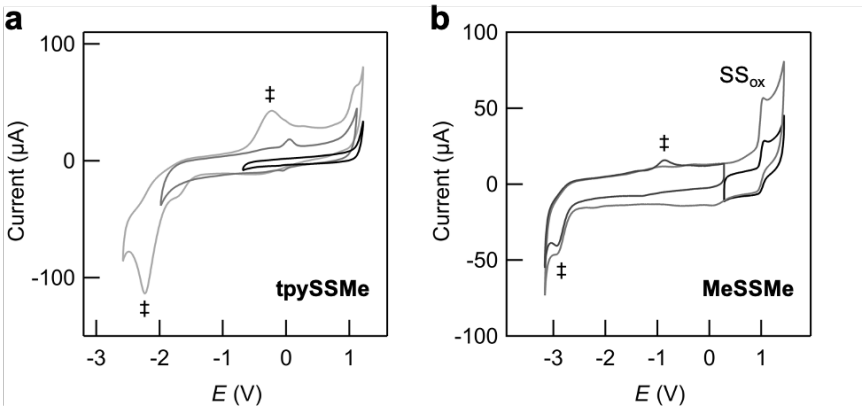

Figure S3. Representative overlaid solution cyclic voltammograms of **(a) tpySSMe** in CH_2Cl_2−0.1 M Bu_4NPF_6 and **(b)** dimethyldisulfide (**MeSSMe**) in MeCN−0.1 M Bu_4NPF_6. Potentials for voltammograms without redox features are adjusted relative to other voltammograms obtained during the same experiment, and may exhibit errors up to ±0.1 V due to reference potential drift. Redox features marked by double-daggers (‡) are attributed to the reduction of the disulfide group (SS_{red}), followed by oxidation of the resulting thiolate(s) to thiyl radicals (S^{-}_{ox}, **Figure 3e**).[17] For **MeSSMe**, the oxidation feature marked by "SS_{ox}" is attributed to the formation of a disulfide radical cation (R−$SS^{+\cdot}$−R).

Table S10. Selected electrochemical parameters for disulfide-based redox processes.[a]

entry	complex	$E_{(SSred)}$	$E_{(S-ox)}$ [b]	$E_{(SSox)}$	$E_{(*,ox)}$	$E_{(*,red)}$
1	[Fe(**tpySSMe**)$_2$][PF_6]$_2$	−1.529	(−0.31)	-	1.021	−1.079
2	[Co(**tpySSMe**)$_2$][PF_6]$_2$	−1.07 [c]	(0.52)	-	1.036	−0.898
3	[Zn(**tpySSMe**)$_2$][PF_6]$_2$	−1.542	(0.37)	-	1.040	−1.111
5	**tpySSMe** [d]	−2.236	−0.247	-	-	-
			(−0.63)			
6	**MeSSMe**	−2.928	−0.869	1.029	-	-
			(−1.07)	-	-	-

[a] Conditions: scan rate 1 V s^{-1}; working electrode, glassy carbon; reference and counter electrodes, Pt; electrolyte, MeCN−0.1 M Bu_4NPF_6, unless otherwise stated. All potentials in V, corrected for iR_s and reported relative to FcH/$[FcH]^+$. [b] Obtained from voltammograms extending to reduction potentials below the SS_{red} feature. Values in parentheses are the onset potential. [c] Onset potential. [d] Measured in CH_2Cl_2–0.1 M Bu_4NPF_6 due to the poor solubility of this compound in MeCN.

Table S11. Selected electrochemical parameters for **MSS**, and **CoSH** SAMs.[a]

entry	SAM (ratio/conditions)	$M^{2+/3+}$	$E_{1/2}$	ΔE_p	E_{pa}	E_{pc}	I_{pa}/I_{pc}[b]	E_{FWHM} [c]	**Γ** (pmol/cm^2) [c]
1	**FeSS**	Fe	0.823	0.080	0.863	0.783	0.61	0.191	33.85
2	**CoSS**	Co	−0.105	0.060	−0.075	−0.135	0.92	0.211	39.46 [d]
3	**CoSS** (N_2) [e]	Co	−0.108	0.042	−0.087	−0.129	0.85	0.232	52.29
4	**CoSH** (N_2) [e]	Co	−0.072	0.042	−0.051	−0.093	0.84	0.180	39.88
5	**CoSS** (Au-on-glass) [f]	Co	−0.085	0.126	−0.022	−0.148	0.78	0.332	43.50

[a] Conditions: scan rate 1 V s^{-1}; working electrode, chemically modified Au disc; reference and counter electrodes, Pt; electrolyte, CH_2Cl_2−0.1 M Bu_4NPF_6, unless otherwise stated. All potentials in V, corrected for iR_s and reported relative to FcH/[FcH]$^+$. $\Delta E_p = | E_{pa} - E_{pc} |$. [b] We attribute deviations from $I_{pa}/I_{pc} = 1$ for **MSS** and **MSH** SAMs to difficulties in accurately fitting baselines to these low intensity voltammogram peaks, particularly for peaks close to the onset of solvent oxidation. [c] Average full width at half maximum (E_{FWHM}) and surface coverage (**Γ**) obtained by analysis of both oxidation and reduction waves. [d] Average from 6 electrodes. [e] SAMs prepared under N_2 in a glovebox. [f] SAMs prepared on "as deposited" gold-on-glass substrates with a geometric area of 1.1 cm^2. Potentials reported for scan rate 0.1 V s^{-1}.

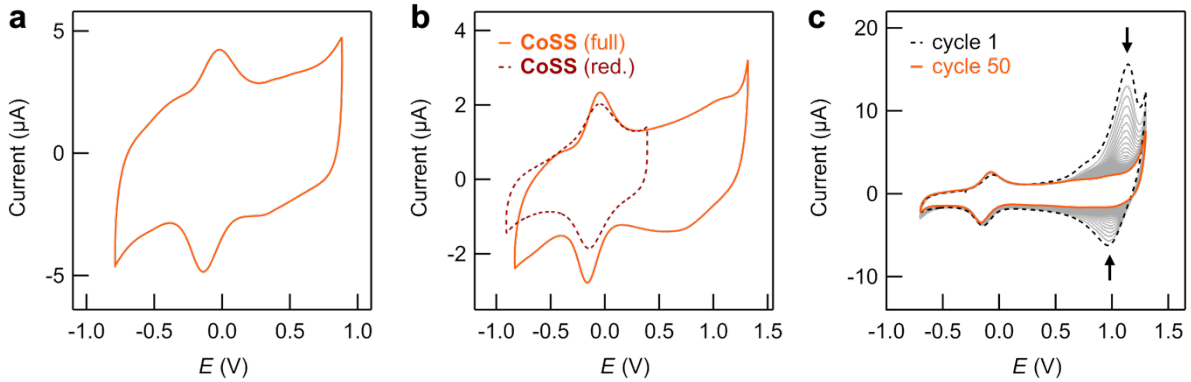

Figure S4. (a) A cyclic voltammogram obtained for a **CoSS** SAM formed on a freshly evaporated gold-on-glass substrate, with potentials corrected for iR_s. The surface coverage is comparable to SAMs prepared on gold disc electrodes, indicating the surface composition of these SAMs is broadly independent of the electrode surface roughness (**Table S11**). We attribute the high apparent ΔE_p and E_{FWHM} for this SAM (**Table S11**) to uncompensated resistances associated with the use of a large area working electrode in CH_2Cl_2-0.1 M Bu_4NPF_6. **(b)** Overlaid cyclic voltammograms for the same **CoSS** SAM as shown in **Figure 4b**, scanned to different potentials. The double-layer capacitance of these modified electrodes is reduced when scanning to potentials below the oxidative limit (extended potential range voltammogram reproduced from **Figure 4b** for convenience). **(c)** We plot representative overlaid surface cyclic voltammograms measured in CH_2Cl_2–0.1 M Bu_4NPF_6 for a SAM formed from an acetone solution of a **CoSS** sample prepared using method A (cycle 1 = black dotted, cycle 50 = orange solid). A distinct irreversible oxidation feature is observed that disappears upon repeated potential cycling. These voltammograms are representative of SAMs formed from solutions of this **CoSS** sample in MeCN for ≥18 h or 2 h, from a MeCN solution of $\mathbf{CoSS^{3+}}$ prepared from this **CoSS** sample, or for analogous SAMs measured in MeCN–0.1 M Bu_4NPF_6. No obvious impurities were observed by ^{1}H NMR spectroscopy, and elemental analysis of this sample agreed with the calculated CHN% values.

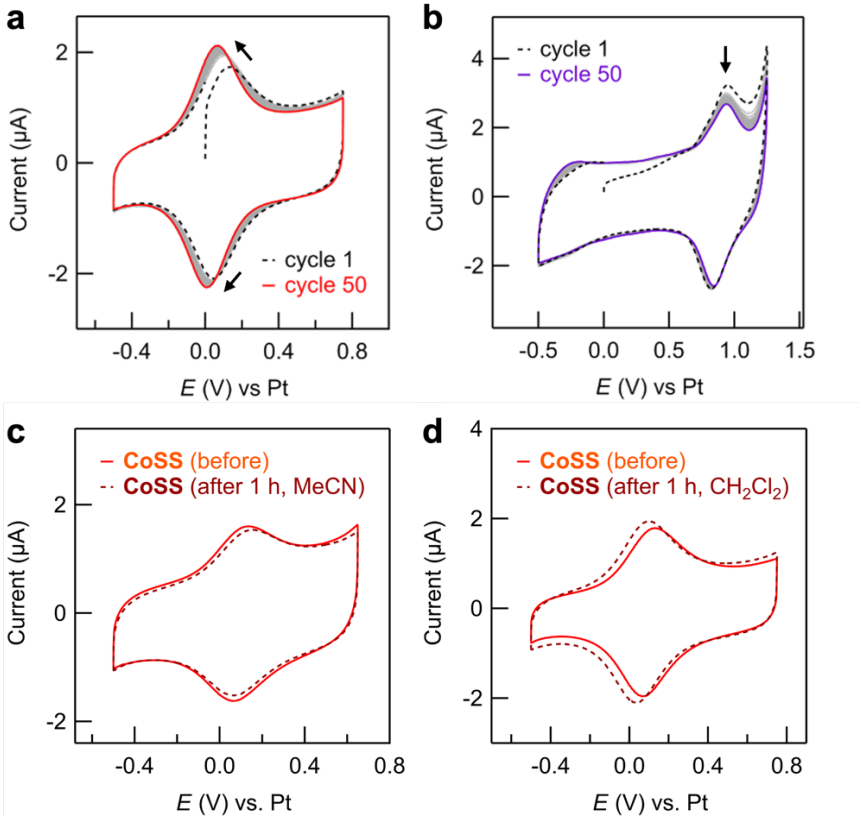

Figure S5. (a, b) Overlaid cyclic voltammograms for **CoSS** and **FeSS** SAMs, respectively, showing the current response upon repeated potential cycling in CH_2Cl_2 (cycle 1 = black dotted; cycle 100 = orange/purple solid). No significant reduction in the peak intensity is observed, indicating these SAMs are stable upon repeated oxidation/reduction. **(c, d)** Overlaid cyclic voltammograms for **CoSS**-functionalized electrodes measured before (solid) and after (dotted) immersion for 1 h in CH_2Cl_2 or MeCN, respectively, indicate limited SAM desorption on timescales relevant for electrochemical analyses. Small changes in peak intensity correlate with changes in the double-layer capacitance, suggesting the SAMs may be reorganizing on the surface over time.

7. NMR Spectra

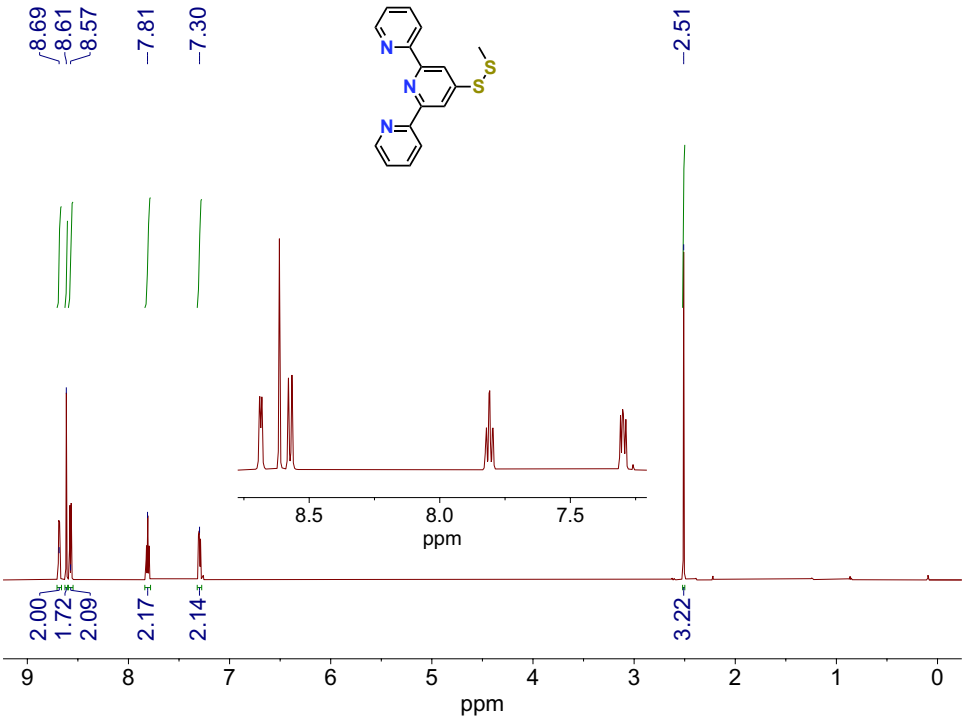

Figure S6. ^{1}H NMR (600 MHz) spectrum of **tpySSMe** in $CDCl_3$.

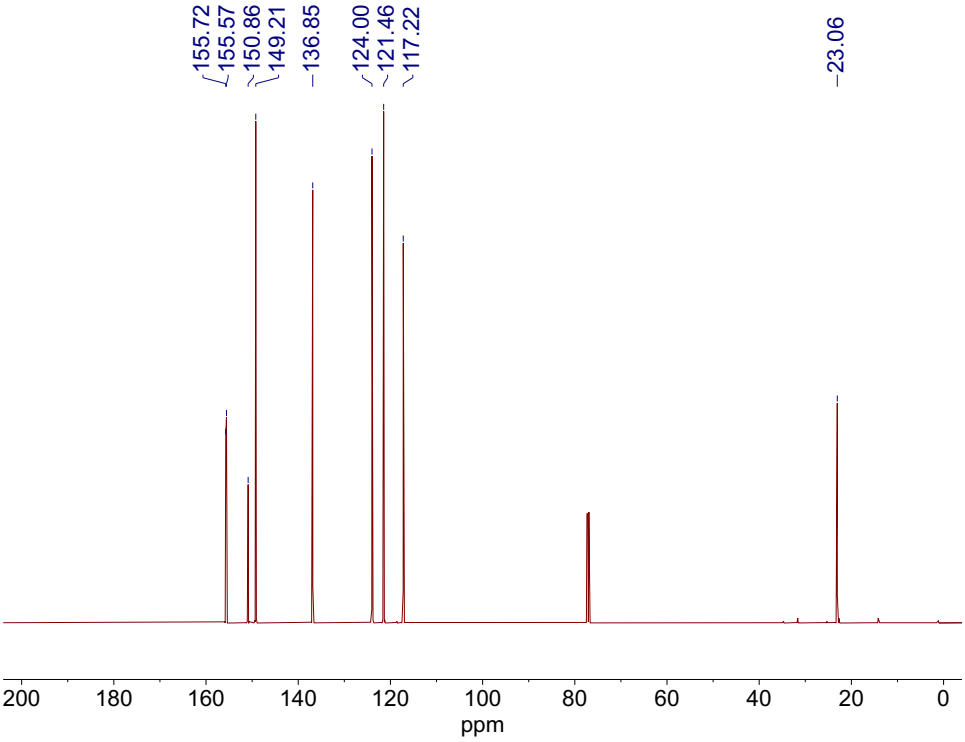

Figure S7. ^{13}C{^{1}H} NMR (150 MHz) spectrum of **tpySSMe** in $CDCl_3$.

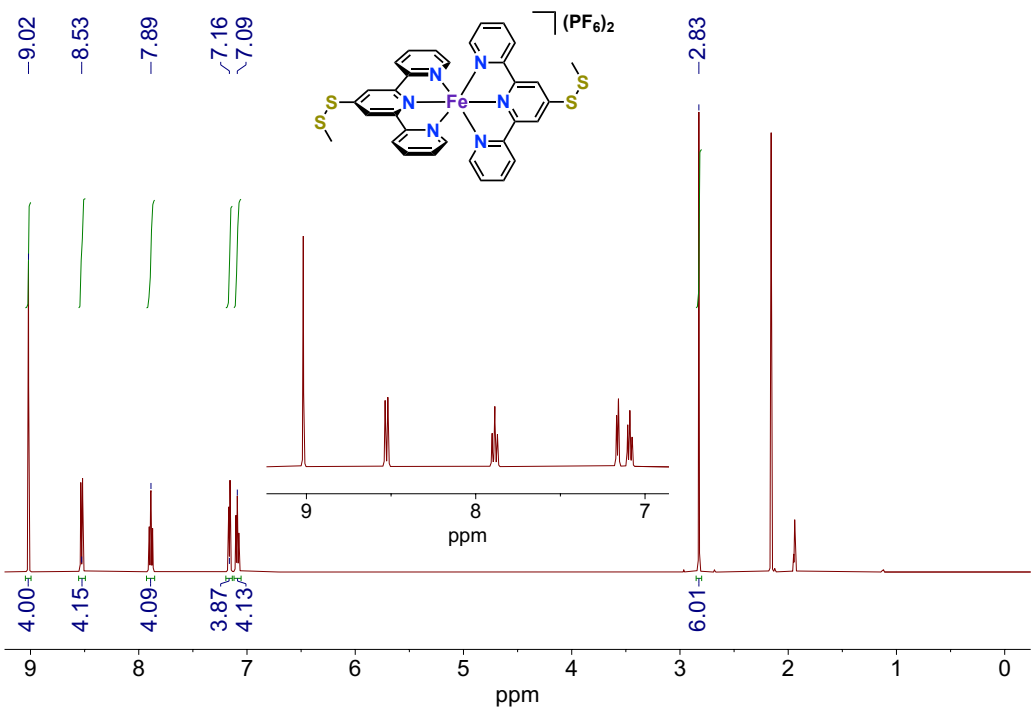

Figure S8. ^{1}H NMR (500 MHz) spectrum of **FeSS** in MeCN-d_3.

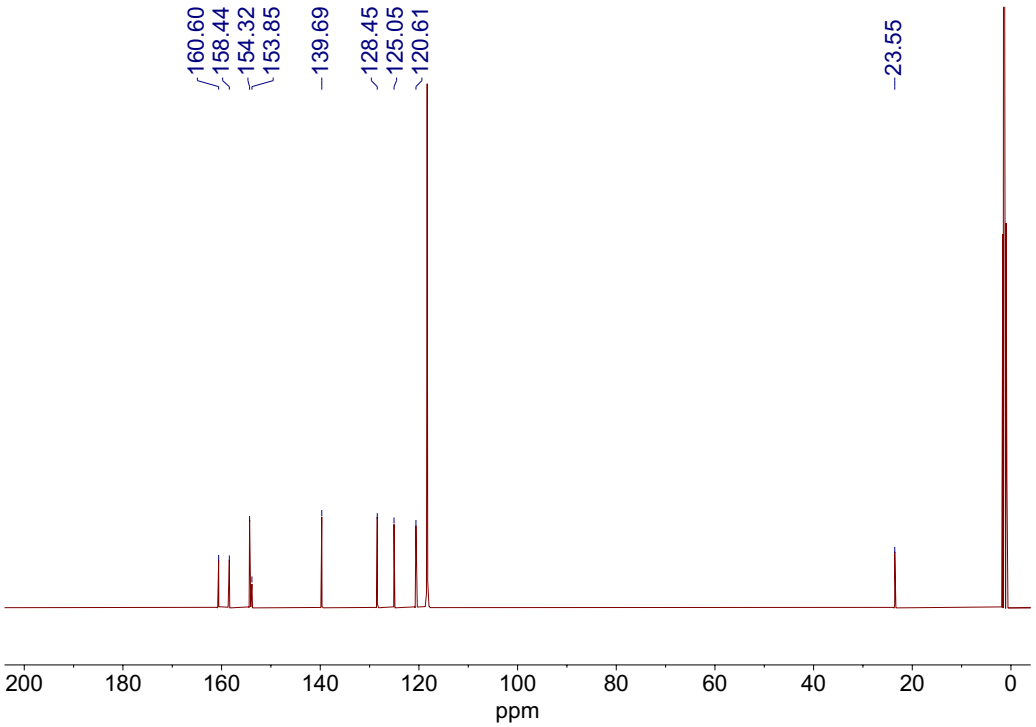

Figure S9. ^{13}C{^{1}H} NMR (125 MHz) spectrum of **FeSS** in MeCN-d_3.

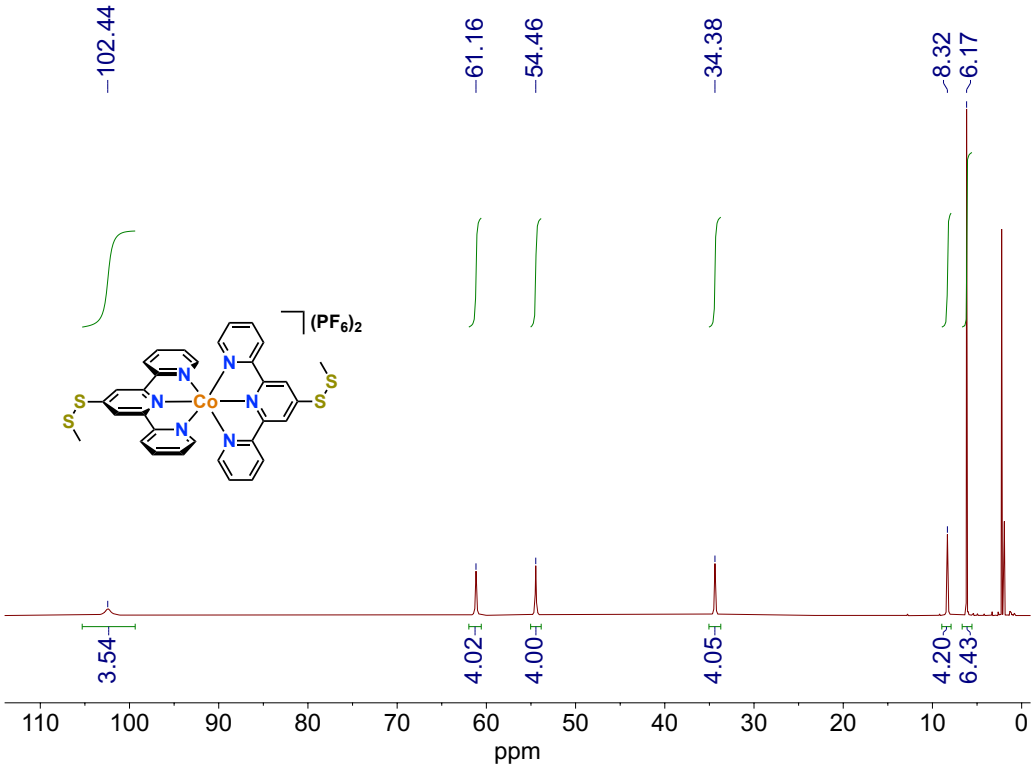

Figure S10. ^{1}H NMR (400 MHz) spectrum of **CoSS** in MeCN-d_3.

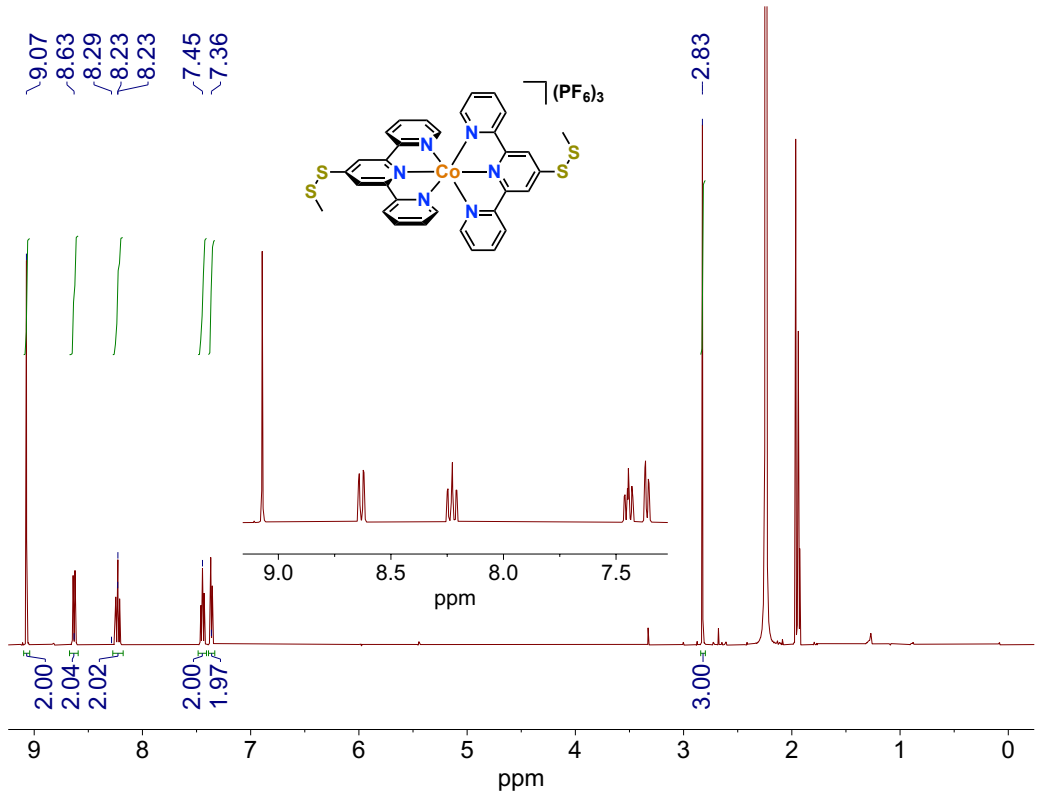

Figure S11. ^{1}H NMR (400 MHz) spectrum of **CoSS^{3+}** in MeCN-d_3.

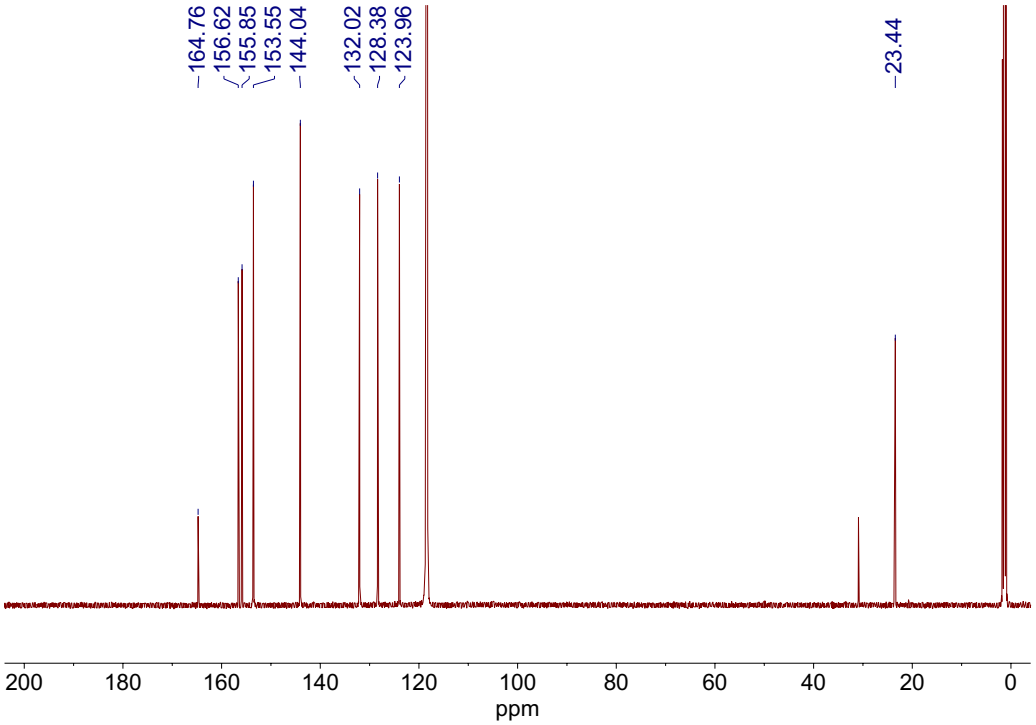

Figure S12. $^{13}C\{^{1}H\}$ NMR (150 MHz) spectrum of **CoSS**$^{3+}$ in MeCN-d_3.

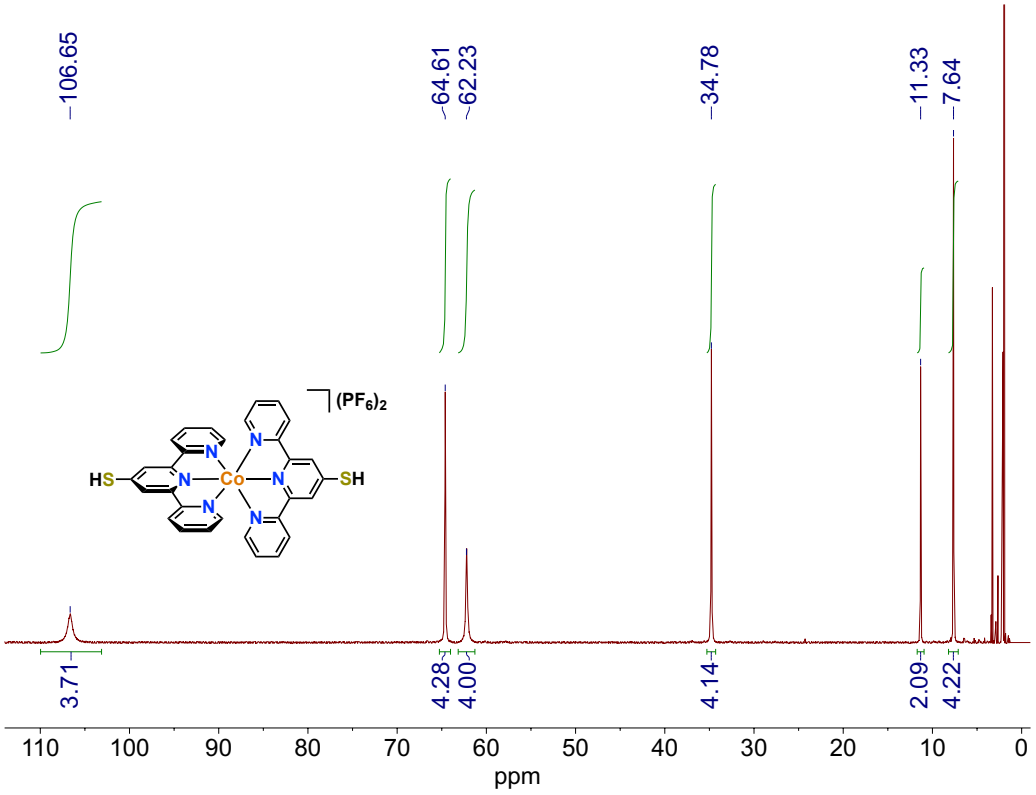

Figure S13. ^{1}H NMR (500 MHz) spectrum of **CoSH** in MeCN-d_3 (under N_2 atmosphere).

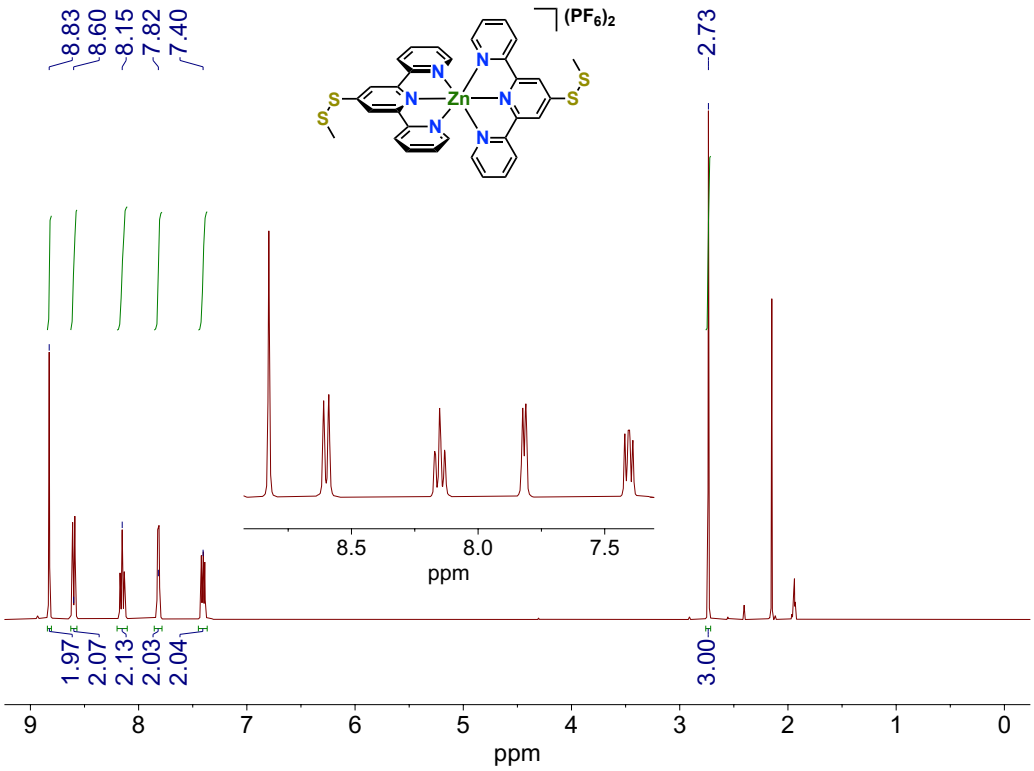

Figure S14. ^{1}H NMR (600 MHz) spectrum of **ZnSS** in MeCN-d_3.

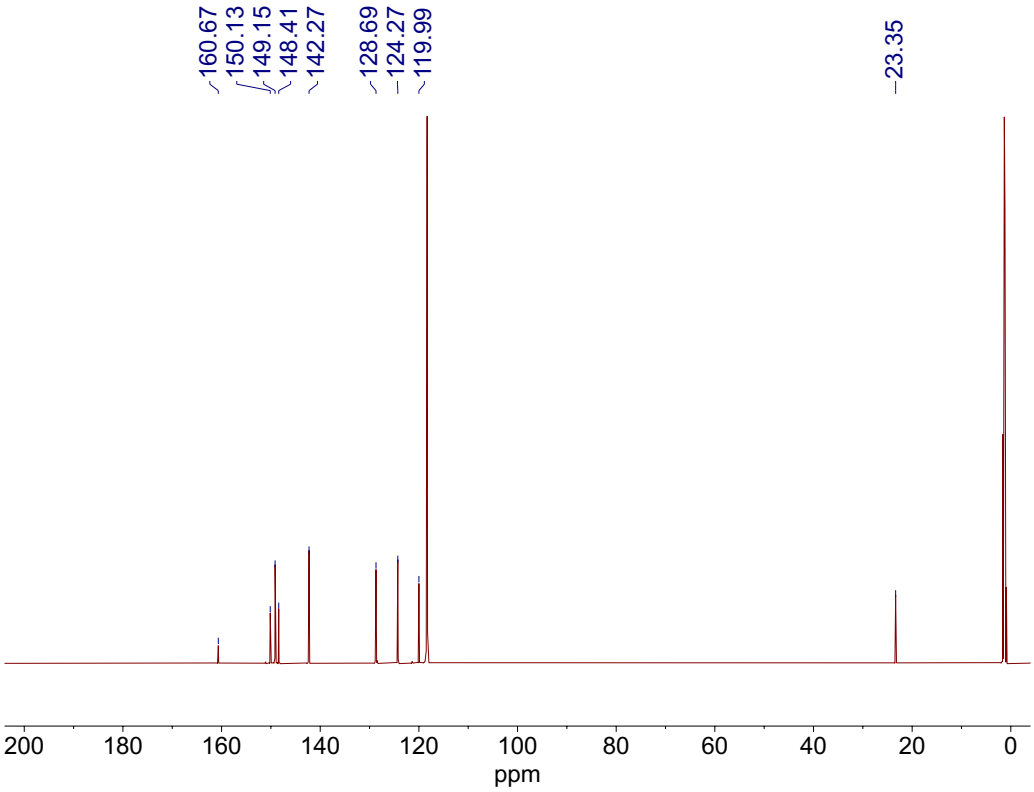

Figure S15. ^{13}C{^{1}H} NMR (150 MHz) spectrum of **ZnSS** in MeCN-d_3.

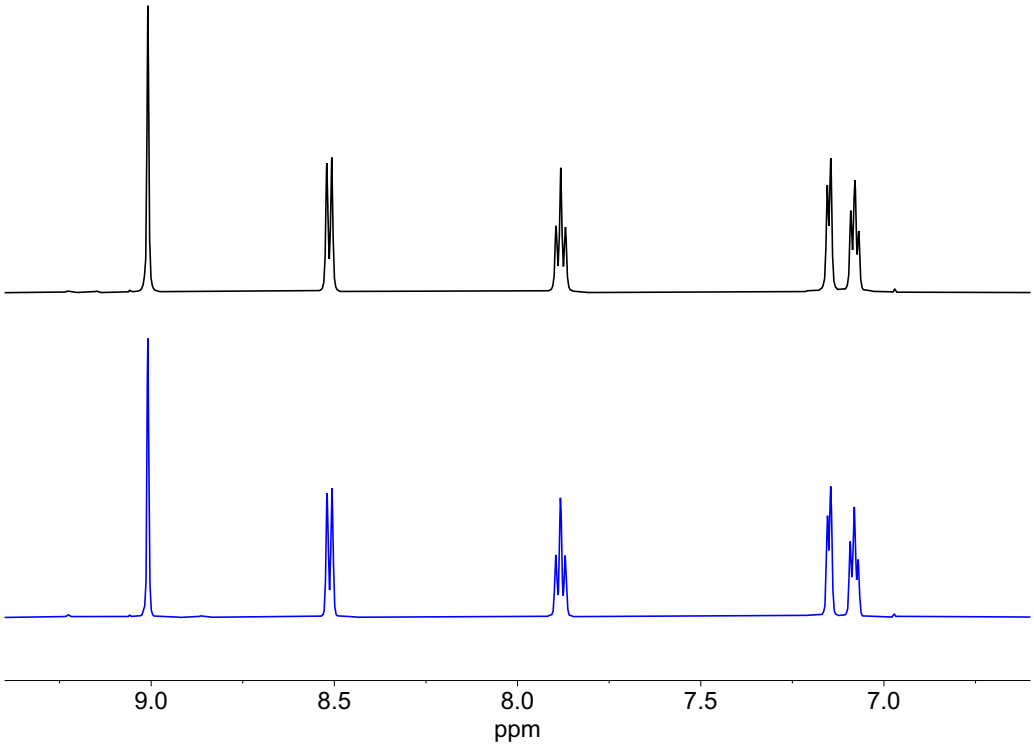

Figure S16. Stacked ^{1}H NMR (600 MHz) spectra for **FeSS** in MeCN-d_3 measured in air, expanded to show the aromatic region. The spectrum obtained after 7 d (*bottom*) shows no discernible changes compared to the initial spectrum (*top*). This confirms that **FeSS** exhibits a higher solution stability relative to **FeSH**, which is reported to form disulfide-bridged multinuclear complexes in air after 1 d.[18]

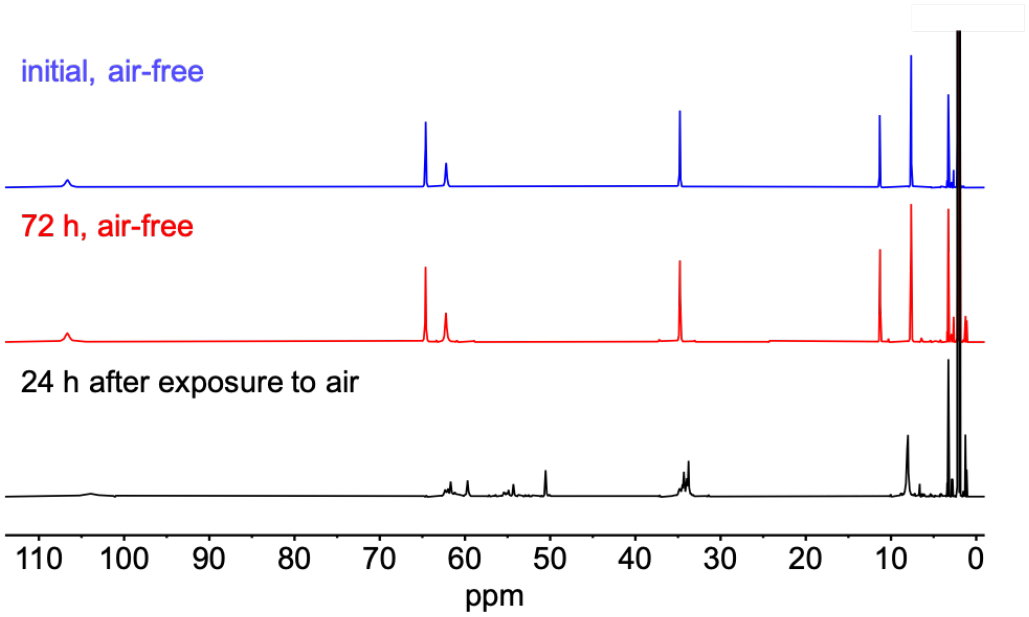

Figure S17. Stacked ^{1}H NMR spectra (500 MHz) for **CoSH** in MeCN-d_3. No significant spectral changes are observed after 72 h (blue, red) for a sample prepared in the glovebox and stored in a sealed NMR tube, indicating **CoSH** does not readily decompose in air-free solution. A processed spectrum is shown in **Figure S11**. After exposure of the same sample to air for 24 h, substantial changes to the characteristic **CoSH** ^{1}H NMR resonances are observed providing strong evidence of the compound's rapid decomposition (black, bottom).

8. References

(1) Fulmer, G. R.; Miller, A. J. M.; Sherden, N. H.; Gottlieb, H. E.; Nudelman, A.; Stoltz, B. M.; Bercaw, J. E.; Goldberg, K. I. NMR Chemical Shifts of Trace Impurities: Common Laboratory Solvents, Organics, and Gases in Deuterated Solvents Relevant to the Organometallic Chemist. *Organometallics* **2010**, *29*, 2176–2179.

(2) SHELXTL 2014/7, Bruker AXS, Madison, WI, 2014.

(3) Sheldrick, G. M. SHELX-97. *Acta Crystallogr., Sect. A* **2008**, *64*, 112–122.

(4) Sheldrick, G. M. Crystal Structure Refinement with SHELXL. *Acta Crystallogr., Sect. C* **2015**, *71*, 3–8.

(5) Hübschle, C. B.; Sheldrick, G. M.; Dittrich, B. ShelXle: A Qt Graphical User Interface for SHELXL. *J. Appl. Crystallogr.* **2011**, *44*, 1281–1284.

(6) CrysAlisPro. Rigaku, V1.171.41.120a, 2021.

(7) Ron, H.; Matlis, S.; Rubinstein, I. Self-Assembled Monolayers on Oxidized Metals. 2. Gold Surface Oxidative Pretreatment, Monolayer Properties, and Depression Formation. *Langmuir* **1998**, *14*, 1116–1121.

(8) Trasatti, S.; Petrii, O. A. Real Surface Area Measurements in Electrochemistry. *J.Electroanal. Chem.* **1992**, *327*, 353–376.

(9) Zuliani, C.; Walsh, D. A.; Keyes, T. E.; Forster, R. J. Formation and Growth of Oxide Layers at Platinum and Gold Nano- and Microelectrodes. *Anal. Chem.* **2010**, *82*, 7135–7140.

(10) Constable, E. C.; Hermann, B. A.; Housecroft, C. E.; Neuburger, M.; Schaffner, S.; Scherer, L. J. 2,2′:6,2″-Terpyridine-4′(1′H)-Thione: A Missing Link in Metallosupramolecular Chemistry. *New J. Chem.* **2005**, *29*, 1475–1481.

(11) Kitson, T. M.; Loomes, K. M. Synthesis of Methyl 2- and 4-Pyridyl Disulfide from 2- and 4-Thiopyridone and Methyl Methanethiosulfonate. *Anal. Biochem.* **1985**, *146*, 429–430.

(12) Harzmann, G. D.; Neuburger, M.; Mayor, M. 4,4″-Disubstituted Terpyridines and Their Homoleptic Fe^{II} Complexes. *Eur. J. Inorg. Chem.* **2013**, *2013*, 3334–3347.

(13) Constable, E. C.; Housecroft, C. E.; Kulke, T.; Lazzarini, C.; Schofield, E. R.; Zimmermann, Y. Redistribution of Terpy Ligands—Approaches to New Dynamic Combinatorial Libraries. *J. Chem. Soc. Dalt. Trans.* **2001**, No. 19, 2864–2871.

(14) Chambers, J.; Eaves, B.; Parker, D.; Claxton, R.; Ray, P. S.; Slattery, S. J. Inductive

Influence of 4′-Terpyridyl Substituents on Redox and Spin State Properties of Iron(II) and Cobalt(II) Bis-Terpyridyl Complexes. *Inorganica Chim. Acta* **2006**, *359*, 2400–2406.

(15) Gryko, D. T.; Clausen, C.; Roth, K. M.; Dontha, N.; Bocian, D. F.; Kuhr, W. G.; Lindsey, J. S. Synthesis of "Porphyrin-Linker-Thiol" Molecules with Diverse Linkers for Studies of Molecular-Based Information Storage. *J. Org. Chem.* **2000**, *65*, 7345–7355.

(16) Dickenson, J. C.; Haley, M. E.; Hyde, J. T.; Reid, Z. M.; Tarring, T. J.; Iovan, D. A.; Harrison, D. P. Fine-Tuning Metal and Ligand-Centered Redox Potentials of Homoleptic Bis-Terpyridine Complexes with 4′-Aryl Substituents. *Inorg. Chem.* **2021**, *60*, 9956–9969.

(17) Borsari, M.; Cannio, M.; Gavioli, G. Electrochemical Behavior of Diphenyl Disulfide and Thiophenol on Glassy Carbon and Gold Electrodes in Aprotic Media. *Electroanalysis* **2003**, *15*, 1192–1197.

(18) Van Der Geer, E. P. L.; Van Koten, G.; Klein Gebbink, R. J. M.; Hessen, B. A [4Fe-4S] Cluster Dimer Bridged by Bis(2,2′:6′,2″- Terpyridine-4′-Thiolato)Iron(II). *Inorg. Chem.* **2008**, *47*, 2849–2857.